

## ORR STUDY ON Fe- AND Co- DOPED MANGANESE DIOXIDE WITH RAMSDELLITE STRUCTURE

ZUDINA L.V.<sup>a)</sup>, SOKOLSKY G.V.<sup>a)</sup>, BOLDYREV E.I.<sup>b)</sup>,  
GAIUK N.V.<sup>c)</sup>

<sup>a)</sup>*National University of Food Technologies, Kyiv, Ukraine*

<sup>b)</sup>*V.I. Vernadsky Institute of General and Inorganic Chemistry of NASU, Kyiv, Ukraine*

<sup>c)</sup>*Bila Tserkva National Agrarian University, Ukraine*  
*gvsokol@rambler.ru*

Oxygen reduction reaction (ORR) belongs to intensively studied electrocatalytic processes from the point of view of its fundamental and practical significance. Recent developments in Li-air battery (LAB) and fuel cell technologies area demand a new insight into air electrode construction and characteristics including bifunctionality of oxygen electrocatalyst for ORR and OOR (oxygen oxidation reaction). Manganese dioxide has long application as an air electrode and is supposed to be promising as an active layer of the air electrode in LAB. The electrolytic doping procedure can be successfully applied to induce phase composition changes and to incorporate active sites of defect redox pairs  $M^{n+1}/M^{n+}$  of various nature in the oxide matrix. Manganese dioxide doped by Fe(II) and Co(II) electrolytically is studied as an air electrode in alkaline electrolyte. Both oxides belong to so-called  $\gamma$ - $MnO_2$  with ramsdellite structure. ORR was studied by the CVA method comparing with  $NH_4^+$ -doped  $MnO_2$  with hollandite structure. It can be concluded that electrolytic doping influences the mechanism of ORR (OOR) process. The nature of this influence is discussed. It can be pointed out that Fe(II) and Co(II) additives studied are promising instruments of manganese dioxide bifunctionality in ORR (OOR). The Tafel slope observed on doped  $MnO_2$  electrodes for ORR is in agreement with platinum electrode reference data of 60 and 120 mV/dec.

The pioneering developments of practical application of oxygen electrocatalysis regarding power sources and fuel cells for the last decade have renewed attention of researchers to fundamentals of oxygen electrocatalysis [1, 2]. Li-air battery (LAB) technology combines advantages of Li-ion batteries with cheap and effective work of air-electrodes ( $O_2$  as an active material is supplied by the diffusion through the hole in the battery can) [1]. The lithium–air cell with a promising lanthanum–lithium titanate ceramic electrolyte [3] demand further

improvements of the catalytic air electrode material. The main criterion for its choice should be not only oxygen reduction activity but ability to support oxygen formation in the reverse direction by oxidation of oxygen anion.

There is an interest in oxide compounds of manganese as one of the most effective oxygen electrocatalyst alternative to noble metals [4, 5]. The best activity for promising Li-air battery (LAB) technology is shown by the  $\alpha$ -polymorph of  $\text{MnO}_2$  with nanowire morphology demonstrating a capacity of  $3000 \text{ mAhg}^{-1}$  [2]. The crystal structure of the  $\alpha$ -polymorph is that of hollandite and consists of  $2 \times 2$  tunnels formed by edge- and corner-sharing  $\text{MnO}_6$  octahedra with the ability to accommodate both  $\text{Li}^+$  and  $\text{O}^{2-}$  or  $\text{O}_2^{2-}$  in the case of aqueous or non-aqueous types of LAB.

As shown in recent publications [6, 7], the redox pairs of  $\text{Mn(III)/Mn(IV)}$ , Jahn-Teller distorted  $\text{Mn(III)}$  ions of surface layer of the crystal lattice are the most probable active sites of oxygen reduction and oxygen oxidation reactions (ORR (OOR)). In addition,  $\text{Mn}_2\text{O}_3$  prominent activity as an air electrode was established recently [7]. Therefore, not only manganese oxides with hollandite structure should be studied.

Electrodeposition belongs to the low temperature synthesis method with nonstoichiometric nature of electrodeposited products that are usually active (electro) catalysts and electrode materials. The electrolytic doping procedure developed in our research group [8] can be an instrument of functionalization of an electrodeposited product. The dopant ions present during the electrocrystallisation process in an electrolyte attract attention, especially their capability to heterovalent substitution of manganese in the host structure.

The doping ions having different mechanism of incorporation into the crystal lattice or role during the electrocrystallisation process cause various changes in the phase composition of the product. The manganese oxide materials electrodeposited in the presence of  $\text{Fe}^{2+}$  and  $\text{Co}^{2+}$  ions were under investigation in this study.

### **Research Methodology**

The pristine fluorine-containing electrolyte consisted of  $0.1 \text{ M HF} + 0.7 \text{ M MnSO}_4$  [9]. The dopant additives in the electrolyte were  $0.01 \text{ M (Fe}^{2+})$ ,  $0.01 \text{ M (Co}^{2+})$ . Samples produced in the presence of  $0.01 \text{ M (Cr}^{3+})$ , and  $1.5 \text{ M NH}_4^+$  additives were also taken for comparison purposes. The electrosynthesis was performed on the platinum anode (at a current density ( $j$ ) of  $10 \text{ A/dm}^2$ ) using the glass-carbon plate as an auxiliary electrode. All the chemical reagents used were of grade AR or higher.

The elemental analysis was carried out by the atomic absorption spectroscopy (AAS) method. The X-ray analyses were performed on a DRON-4 instrument ( $\text{CuK}_\alpha$ -radiation) with computer interface. XRD

patterns were registered also on MoK $\alpha$ -irradiation to improve the signal/noise ratio. The preliminary processing of X-ray patterns included smoothing, background subtraction and normalization according to the procedure described earlier. The simulations of XRD patterns by the Rietveld refinement method were made using a Powder Cell v. 2.3 package [10, 11]. Diffusion peaks of XRD patterns were successfully interpreted by the Rietveld refinement as a set of phase components detected in samples with sizes of crystallites lower than the XRD detection limit (about 5 nm).

The cyclic voltammetry (CVA) experiment was carried out in a standard three electrode cell using 0.3 M LiOH (KOH) electrolyte saturated with O<sub>2</sub> (air, Ar). The voltammograms were taken with an IPC-PRO potentiostat–galvanostat with computer interface at potential change rates of 0.001–0.5 V/s. Glass carbon plate was an auxiliary electrode. Carbon paste electrode (CPE) was a thoroughly grounded mixture of doped manganese oxide: graphite in the ratio 70 : 30 and polytetrafluoroethylene (PTFE) emulsion loaded into PTFE-tube. The Luggin capillary was also used by standard procedure.

## Results and Discussion

The iron (II) ion additive has an experimentally verified positive influence on manganese dioxide activity to phenol degradation [8]. The simultaneous action of manganese dioxide and the Fe (III)/Fe (II) redox pair at the anode phenol oxidation is in agreement with the action of Fenton reagent [8]. The oxidation process activity is prospective for application in OOR taking into account high activity of manganese dioxide in ORR. The cobalt (II) ion additive can improve catalytic activity of H<sub>2</sub>O<sub>2</sub> decomposition by the electrodeposition product. It was shown earlier that cobalt oxide-hydroxides electrodeposited from fluorine-containing electrolytes are the most active H<sub>2</sub>O<sub>2</sub> decomposition catalysts found by us in addition to higher standard electrode potential of the Co (III)/Co (II) redox pair compared with manganese dioxide [8].

The high current density of 10 A/dm<sup>2</sup> used suggests crystallite growth conditions controlled by the bulk diffusion of Mn(II) ions from the electrolyte. The high rate of nuclei formation defines the kinetics of electrodeposition of powdered samples with rod-like nanocrystallites. TEM and SEM measurements showed rods length to be within 100–400 nm and of 5–25 nm in diameter.

XRD-study was carried out to determine the phase composition and to evaluate the size of coherent scattering domains using Powder Cell package. The size of these domains is consistent with SEM and TEM data. The XRD phase analysis showed the following main phase components depending on dopants added:  $\gamma$ -MnO<sub>2</sub> (ramsdellite, Pbam) — Fe<sup>2+</sup>;  $\gamma$ -MnO<sub>2</sub> (ramsdellite, Pbam) — Co<sup>2+</sup>;  $\delta$ -MnO<sub>2</sub> (birnessite, C2/m)

—  $\text{Cr}^{3+}$ .  $\alpha\text{-MnO}_2$  (hollandite,  $I4/m$ ) —  $\text{NH}_4^+$ . It can be concluded that low charged transition metal ions stabilise the ramsdellite structure type, whereas the  $\text{Cr}^{3+}$  ion induces formation of the  $\delta$ -polymorph with a layered structure “pillared” by these ions. These results are in agreement with thermodynamics of aforementioned phases were structure channels and defects states have significant energy gain when they are stabilised by the  $\text{M}^+$  dopants or water molecules [12].

CVAs of doped  $\text{MnO}_2$  CPE in 0.50 M LiOH solution saturated with oxygen are shown in Figure 1. The distinct features of potential window in aqueous alkaline electrolyte are the reduction and oxidation processes of manganese dioxide observed at negative potentials (vs  $\text{AgCl}|\text{Ag}^0$ ) and peaks of ORR that appear after saturation of the electrolyte with oxygen or after prolonged anode polarisation attended by oxygen evolving (OOR, Figure 2). There are usually two weak steps of ORR in the  $\mu\text{A}$  range of current, and after saturation with oxygen gas they become visible in the mA range of currents (Fig. 2). Both steps are detectable at low rates of potential scan (below  $75\text{mV}\cdot\text{s}^{-1}$ ) since oxygen reduction kinetics is very slow. It is not the case of hydrogen peroxide that is the expected intermediate of oxygen reduction and better detectable at scan rates range of  $100\text{-}300\text{ mV}\cdot\text{s}^{-1}$ . OOR is observed at more than  $1000\text{ mV}$  (Fig. 2).

To study  $\text{H}_2\text{O}_2$  behaviour, the CVA of the same electrolyte with  $\text{H}_2\text{O}_2$  additive of different concentrations was examined. The  $\text{H}_2\text{O}_2$  response on CVA can be seen near  $500\text{ mV}$ s of the reverse scan of CVA curve. The dependence of this peak current on  $\text{H}_2\text{O}_2$  concentration is prospective for sensor applications. On the other hand, we observed peroxide decomposition onto the electrode surface in the same electrolyte without current since manganese dioxide is an active catalyst of  $\text{H}_2\text{O}_2$  decomposition in aqueous medium.

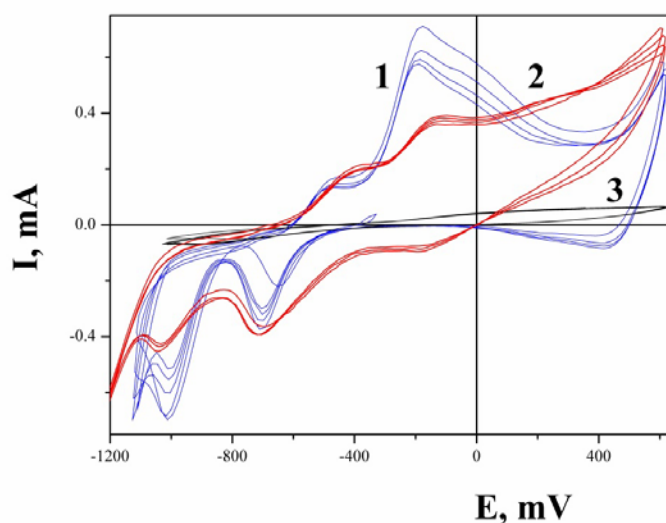


**Fig. 1.** CVA of  $\text{NH}_4^+$  (1),  $\text{Co}^{2+}$  (2)- doped manganese(IV) oxide and graphite (3) electrodes in saturated by  $\text{O}_2$  0.3 M KOH electrolyte solution ( $V = 10\text{ mV}\cdot\text{s}^{-1}$ ).

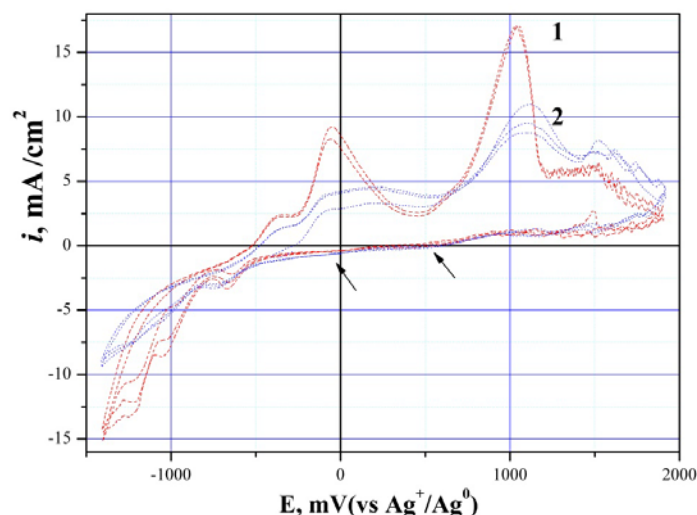


**Fig. 2.** CVA of Fe-doped  $\gamma$ -MnO<sub>2</sub> sample CPE in O<sub>2</sub> saturated 0.3M LiOH: 1 —  $V = 20 \text{ mV}\cdot\text{s}^{-1}$ ; 2 —  $V = 75 \text{ mV}\cdot\text{s}^{-1}$  (Arrows indicate two steps of dioxygen reduction).

In general, ORR is a complex multi-electron process and its mechanism is under thorough investigation. Some of the mechanisms have no hydrogen peroxide as an intermediate. For instance, the dissociative mechanism that was proposed by Density Functional Theory calculations [13] includes dissociative adsorption of oxygen and its further reaction with proton and electron, and OH<sub>ads</sub> again reacts with H<sup>+</sup> and e<sup>-</sup> forming water as well as direct 4e<sup>-</sup> electron transfer is shown in some cases on the Pt electrode [13].

The similarity with reference data on oxygen reduction in Tafel coordinates on the Pt electrode is shown in Figure 3. Tafel slope  $b$  in case of linear part 1 and 2 is in agreement with 60 and 120 mV on Pt correspondingly.

MnO<sub>2</sub> CPE 1 exhibit two reduction peaks ( $-0.75 \text{ V}$  and  $-1.05 \text{ V}$ , Figure) and two oxidation peaks with slightly resolved shoulder of the third one. Dopant ions induce changes of CVA behaviour of MnO<sub>2</sub> CPE. Co-doped CPE 2 displays additional reduction peak at more electropositive potentials ( $-0.25 \text{ V}$ , Figure1). Fe(II) doped MnO<sub>2</sub> CPE has sharp peak at low scan rates ( $V < 50 \text{ mV}\cdot\text{s}^{-1}$ ) at 1.0 Volts that could be the result of iron (III)/iron (II) redox pair activity, Figure 1. Its growth at low scan rates used in this work was unexpected. We suppose that it could be attributed to cogeneration of oxygen radicals by the Fenton reagent mechanism and their chain reaction transformation. Graphite electrode 4 has by the order of magnitude lower currents of the same processes.

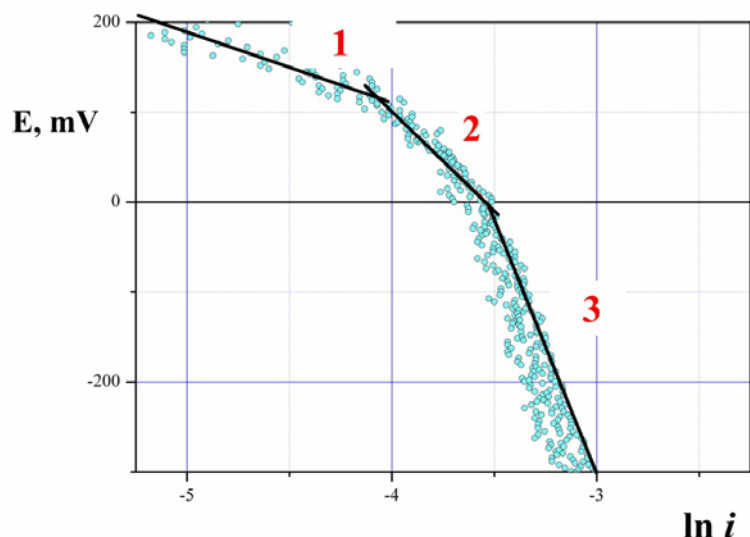


**Fig.3.** Tafel cathode polarisation curves of Fe-doped  $\gamma$ -MnO<sub>2</sub> CPE in O<sub>2</sub> saturated 0.3M LiOH (where 1-2 are the linear regions of oxygen; 3- manganese dioxide reduction).

### Conclusions

The dopant-ions additives in an electrolyte modify the host structure and the interface states of electrodeposited material depending on their nature and electrolysis conditions. The electrolytic doping procedure improves the prospectives of practical application of electrolytic manganese (IV) oxides as electrode materials. The effects of oxygen electrocatalysis in alkaline medium saturated with oxygen (air, argon) were discussed. Both doped by Fe (II) and Co (II) ions samples display some unique features in ORR (OOR). It is stated that combination of Fe (II) and Co (II) additive could be promising for stabilisation of LAB cathode reversibility.

### References

- [1] Scrosati, B., & Garche, J. (2010). Lithium batteries: Status, prospects and future. *Journal of Power Sources*, 195(9), 2419-2430.
- [2] Débart, A., Paterson, A. J., Bao, J., & Bruce, P. G. (2008).  $\alpha$ -MnO<sub>2</sub> Nanowires: A Catalyst for the O<sub>2</sub> Electrode in Rechargeable Lithium Batteries. *Angewandte Chemie*, 120(24), 4597-4600.
- [3] Belous, A. G., Kolbasov, G. Y., Boldyrev, E. I., & Kovalenko, L. L. (2015). Lithium–air cell with lanthanum–lithium titanate ceramic electrolyte. *Russian Journal of Electrochemistry*, 51(12), 1162-1167.

- [4] Matsuki, K., & Kamada, H. (1986). Oxygen reduction electrocatalysis on some manganese oxides. *Electrochimica Acta*, 31(1), 13-18.
- [5] Oh, D., Qi, J., Lu, Y. C., Zhang, Y., Shao-Horn, Y., & Belcher, A. M. (2013). Biologically enhanced cathode design for improved capacity and cycle life for lithium-oxygen batteries. *Nature communications*, 4.
- [6] Ryabova, A. S., Napolskiy, F. S., Tiphaine, P., Istomin, S. Y., Antoine, B., Denis, A., Baranchikov, A. Y., Levin, E. E., Abakumov, A. M., Gw'ena'elle, K., Antipov, E. V., Tsirlina, G. A., and Savinova, E. R. Rationalizing the influence of the mn(iv)/mn(iii) red-ox transition on the electrocatalytic activity of manganese oxides in the oxygen reduction reaction. *Electrochimica Acta* 187 (2016), 161–172.
- [7] Ryabova, A. S., Bonnefont, A., Zagrebin, P., Poux, T., Sena, R. P., Hadermann, J., Abakumov, A. M., Kéranguéven, G., Istomin, S. Y., Antipov, E. V., Tsirlina, G. A., and Savinova, E. R. Study of hydrogen peroxide reactions on manganese oxides as a tool to decode the oxygen reduction reaction mechanism. *CHEMELECTROCHEM* 3, 10 (2016), 1667–1677.
- [8] Sokol'skii, G.V., Ivanova, S.V., Ivanova, N.D. et al. Doped manganese (IV) oxide in processes of destruction and removal of organic compounds from aqueous solutions J. Water Chem. Technol. (2012) 34: 227.
- [9] N.D. Ivanova, E.I. Boldyrev, I.S. Makeeva, G.V. Sokol'skii. Making manganese dioxide from fluorine-bearing electrolytes. Zhurn. Prikl. Khimii 71 (1998) 121-123.
- [10] <http://www.iucr.ac.uk>, programmed by Werner Kraus & Gert Nolze (BAM Berlin), Federal Institute for Materials Research and Testing, Lab. BAM1.33: X-Ray Structure and Phase Analysis.
- [11] W. Kraus, G. Nolze, POWDER CELL — a program for the representation and manipulation of crystal structures and calculation of the resulting X-ray powder patterns. *Journal of Applied Crystallography* vol. 29, 1996, pp. 301-303.
- [12] G.V. Sokolsky, S.V. Ivanov, E. I. Boldyrev et al. // *Solid State Phenom.* 230 85 (2015).
- [13] Song, C., & Zhang, J. (2008). Electrocatalytic oxygen reduction reaction. In *PEM fuel cell electrocatalysts and catalyst layers*, Springer, London, pp. 89-134.